Photodiagnosis and Photodynamic Therapy (2013) xxx, xxx–xxx

Available online at www.sciencedirect.com

SciVerse ScienceDirect

journal homepage: www.elsevier.com/locate/pdpdt

Zinc-pheophorbide *a*—Highly efficient low-cost photosensitizer against human adenocarcinoma in cellular and animal models

Monika Jakubowska[a], Małgorzata Szczygieł[a], Dominika Michalczyk-Wetula[a], Anna Susz[a,b], Grażyna Stochel[b], Martyna Elas[a,*], Leszek Fiedor[a,], Krystyna Urbanska[a]**

[a] *Faculty of Biochemistry, Biophysics and Biotechnology, Jagiellonian University, Gronostajowa 7, Krakow 30-307, Poland*
[b] *Faculty of Chemistry, Jagiellonian University, Ingardena 3, Krakow 30-060, Poland*

KEYWORDS
Zn-pheophorbide;
Human adenocarcinoma;
Photodynamic therapy

Summary
Background: Our previous study has shown a prolonged retention and accumulation of Zn-pheophorbide *a*, a water-soluble derivative of chlorophyll *a*, in tumor tissue (Szczygiel et al. [19]). This prompted us to further evaluate the phototherapeutic potential of this photosensitizer of excellent physicochemical properties.
Methods: Cellular uptake of Zn-pheophorbide, its localization in cells, cytotoxicity, phototoxicity and cell death mechanisms were studied in human adenocarcinoma cell lines: A549, MCF-7 and LoVo. The PDT efficacy was tested against A549 tumors growing in nude mice.
Results: Zn-pheophorbide *a* even at very low concentrations ($\sim 1 \times 10^{-6}$ M) and at low light doses (5 J/cm^2) causes a strong photodynamic effect, leading to 100% cell mortality. Confocal microscopy showed that in contrast to most derivatives of chlorophyll, Zn-pheophorbide *a* does not localize to mitochondria. The photodynamic effects and the cell death mechanisms of Zn-pheophorbide *a*, its Mg analog (chlorophyllide *a*) and Photofrin were compared on the A549 cells. Zn-pheophorbide *a* showed the strongest photodynamic effect, at low dose killing all A549 cells via apoptosis and necrosis. The very high anti-cancer potential of Zn-pheophorbide was confirmed in a photodynamic treatment of the A549 tumors. They either regressed or were markedly inhibited for up to 4 months after the treatment, resulting, on average, in a 5-fold decrease in tumor volume.

* Corresponding author. Tel.: +48 12 664 6338; fax: +48 12 664 6902.
** Corresponding author. Tel.: +48 12 664 6358; fax: +48 12 664 6902.
E-mail addresses: martyna.elas@uj.edu.pl (M. Elas), leszek.fiedor@uj.edu.pl (L. Fiedor).

1572-1000/$ – see front matter
http://dx.doi.org/10.1016/j.pdpdt.2012.12.004

Please cite this article in press as: Jakubowska M, et al. Zinc-pheophorbide *a*—Highly efficient low-cost photosensitizer against human adenocarcinoma in cellular and animal models. Photodiagnosis and Photodynamic Therapy (2013), http://dx.doi.org/10.1016/j.pdpdt.2012.12.004

Conclusion: These results show that Zn-pheophorbide *a* is a very promising low-cost, synthetically easily accessible, second generation photosensitizer against human cancer.

Introduction

The clinical use of photodynamic therapy (PDT) has grown significantly over the past two decades, mainly in cancer, age related macular degeneration (AMD), and skin treatment. Besides the early-generation photosensitizers and popular Photofrin, there are many other clinically approved photosensitizers, such as HpD, Foscan, Levulan, Lutrin, Photochlor and Visudyne that have been successfully employed in PDT in many countries. However, several features of photosensitizers might be considerably improved, leading to much more efficient PDT results. Among them are (i) spectroscopic properties such as high absorption in the red and near infra-red spectrum, (ii) high singlet oxygen yield, (iii) pharmacological properties such as affinity toward tumor tissue and retention time in the organism, and (iv) the ability to modulate the immune response, such as inflammation or tumor-host interactions [1—5]. In light of that, a considerable effort is being made to develop new and better photosensitizers [6,7].

The major photosynthetic pigments, chlorophylls (Chls) and bacteriochlorophylls (BChls), and their derivatives, strongly absorb light in the part of the spectrum coinciding with the therapeutic window of human tissue and in free state are highly efficient generators of singlet oxygen and other reactive oxygen species (ROS) [8,9]. These features, and their natural origin, make them very attractive as photosensitizers. Hence, Chl and BChl derivatives are extensively studied not only for their key functions in photosynthesis but also because of their high potential for applications in photodynamic therapy (PDT) [8,10,11]. To this end, to make these natural pigments suitable for therapeutic purposes, some chemical modifications are necessary, in order, for instance, to increase their solubility in aqueous media as well as to optimize their photophysical properties relevant to PDT [12—14]. Tookad, Pd-substituted bacteriopheophorbide *a*, and its modification Stakel [15—18], are at present among the most clinically advanced tailored chlorophyll derivatives.

Our recent pharmacokinetic study [19] on metallosubstituted chlorophyllides in DBA/2 mice bearing the Cloudman S91 melanoma has shown that the efflux system, probably involving BCRP [20,21], is sensitive to the type of metal ion centrally chelated by the Chl macrocycle. Thus, the pharmacokinetics of Zn-substituted pheophorbide *a* (Zn-Pheide, Fig. 1) is very different from those of the native Mg-derivative. In particular, Zn-Pheide has a longer retention time and reaches higher levels in the tumor. This prompted us to investigate in detail its interactions with the cells and further to evaluate the phototherapeutic potential of Zn-Pheide *in vivo*. Three human adenocarcinoma cell lines (A549, MCF-7 and LoVo), exposed to photodynamic treatment using Zn-Pheide as the photosensitizer, were applied to serve as the experimental *in vitro* model. Our aim was to examine the cellular uptake and localization of Zn-Pheide, and then to compare the responses of the three cell lines to the photodynamic effect. We have also studied the cellular death mechanisms induced by Zn-Pheide and light. The excellent photosensitizing properties of Zn-Pheide are most evident when its PDT efficacy against A549 cells is compared to those of chlorophyllide *a* (Chlide) and Photofrin. Most importantly, the *in vivo* study showed that Zn-Pheide-based PDT led to a complete inhibition of A549 tumors implanted in BALB/cA nude mice. These results show that Zn-Pheide, a synthetically easily accessible and affordable pigment, is a very promising II generation photosensitizer.

Materials and methods

Reagents and solvents

DMEM high glucose, DMEM/F12, MTT [3-(4,5-dimethyltiazol-2-yl)-2,5-diphenyltetrazolim bromide], propidium iodide and eosin Y were purchased from Sigma, Germany; Fetal Calf Serum (FCS) from Gibco, USA; the antibiotics (penicillin, streptomycin) from Polfa Tarchomin, Poland; the Mayer's hematoxylin from Aqua-Med, Poland. The Petri dishes were obtained from TPP, Switzerland; the 96-well plates from Becton Dickinson Biosciences, USA; and the 4-chamber Lab-Tek® Chambered #1.0 Borosilicate Coverglass form NUNC, USA. Acetone was obtained from Eurochem, Poland, dimethyl sulfoxide, ethanol, methanol and formaldehyde were purchased from POCh, Poland — all of analytical grade. Methanol for spectroscopy was obtained from MERCK, Germany.

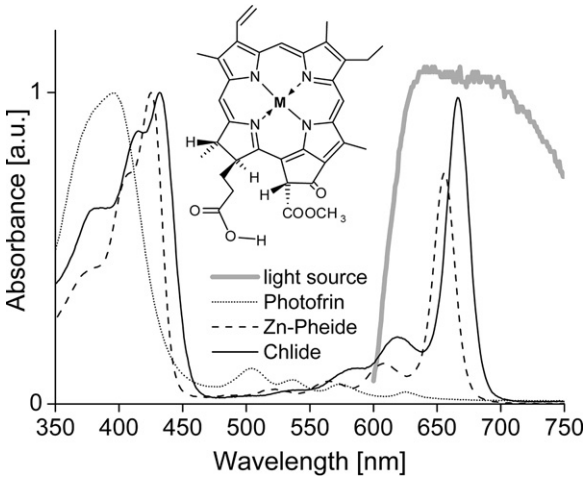

Figure 1 Electronic absorption spectra of Chlide (solid line), Zn-Pheide (dash line), and Photofrin (dotted line) taken in methanol. The spectra were normalized to the intensity of the Soret band. The gray line corresponds to the emission spectrum of the light source used in illuminations. Inset: structural formula of chlorophyllide a and its derivatives (Chlide: M = Mg, Zn-Pheide: M = Zn).

Please cite this article in press as: Jakubowska M, et al. Zinc-pheophorbide *a*—Highly efficient low-cost photosensitizer against human adenocarcinoma in cellular and animal models. Photodiagnosis and Photodynamic Therapy (2013), http://dx.doi.org/10.1016/j.pdpdt.2012.12.004

Equipment

The electronic absorption spectra were recorded on a Cary 50 Bio UV-VIS spectrophotometer, Varian, USA, and the emission spectra on a Perkin-Elmer LS-50B fluorometer, Beaconsfield, UK. The absorbance of MTT formazan was detected using a GENios Plus microplate reader, TECAN, Switzerland. The confocal images were obtained on an Axiovert 200M LSM 510 META confocal microscope equipped with ConfoCor 3 and Plan-Neofluar 40×/1.3 Oil DIC objectives, both from Carl Zeiss MicroImaging GmbH, Germany. The images were analyzed using an LSM Image Browser Version 4.2.0.121 supplied by the manufacturer. Supplementary images were obtained with Leica SMD confocal microscope, using 633 HCX PL APO CS NA 1.4 oil immersion lens (Leica Microsystems GmbH, Wetzlar, Germany); images were analyzed using ImageJ (Rasband, W.S., ImageJ, U.S. National Institutes of Health, Bethesda, MD, http://rsb.info.nih.gov/ij/). All fluorescent probes were purchased from Invitrogen™ (Molecular Probes™, USA). The cell death mechanisms were observed under a Nikon ECLIPSE TS-100F microscope equipped with a UV-2A filter block (excitation 330—380 nm, emission >420 nm), at magnification 100×. The histological images were taken using a Nikon Eclipse Ti microscope (Nikon, Japan), at a magnification of 40 and 100, with image analysis software supplied by the manufacturer. The cells were illuminated using a 150 W fiber optical illuminator, OSH150, (Beijing Tech Instrument Co., Ltd., Shanghai, China), equipped with a cut-off (>600 nm) plastic filter. The light used for the irradiations was characterized spectrally using an IL2000 spectroradiometer, Spectrocube, Germany.

Cell culture

The cell lines (human lung adenocarcinoma epithelial cell line, A549, human breast adenocarcinoma cell line, MCF-7, and human colon adenocarcinoma, LoVo) were kindly provided by Dr. Jolanta Saczko, Wroclaw Medical University, Poland. The cells were cultivated under standard conditions (37 °C, 5% CO_2 in a humid atmosphere). The A549 and MCF-7 cells were cultured in a DMEM high glucose medium supplemented with 10% heat-inactivated FCS and antibiotics. The LoVo cells were cultured in a DMEM/F12 medium supplemented as above.

Photosensitizer

Zn-Pheide and Chlide were prepared from Chla and purified as described previously [19,22]. For estimation of concentrations used for *in vitro* experiments, an aliquot of pigment was dissolved in acetone and the absorption spectra of the solutions were recorded in a 1 cm quartz cuvette at ambient temperature. The concentrations of Chla derivatives were determined photometrically at 663 nm using the extinction coefficient equal to 71,500 $M^{-1}\,cm^{-1}$. After the concentration determination, the pigments were stored dried at −30 °C under Ar atmosphere. Photofrin was the generous gift of Dr. Dominika Nowis, Medical University of Warsaw, Poland. Photofrin (extinction coefficient at 630 nm of 1170 $M^{-1}\,cm^{-1}$ [23]) was dissolved with a cell medium supplemented with FCS to obtain a stock solution (40 μg/ml), which was then stored at −30 °C.

Photosensitizer uptake

24 h before the treatment, 25×10^4 cells were seeded on Petri dishes (ϕ = 40 mm) in 2 ml of a full growth medium and incubated overnight. Solutions of Zn-Pheide at 1×10^{-7}, 2×10^{-7} and 5×10^{-7} M were prepared under dim light by dissolving aliquots of the pigment in ethanol and by diluting in the culture medium (without FCS) so that the final concentration of ethanol was 1%. The cells were rinsed with 2 ml of PBS and then incubated for 2, 6, 12 and 24 h with 2 ml of photosensitizer solution. Afterwards they were rinsed with PBS and suspended in 750 μl acetone on ice. The extracts from two Petri dishes were pooled. Fluorescence emission spectra between 600 and 850 nm of the extracts were recorded, applying excitation at 410 nm. The measurements were done at ambient temperature in 1 cm quartz cuvettes. The number of the cells was estimated according to their doubling time (22, 29 and 33 h for the A549, MCF-7 and LoVo cells, respectively).

Cellular localization of photosensitizers

Cells numbering 15×10^3 were seeded in a 4-chamber Lab-Tek® Chambered #1.0 Borosilicate Coverglass in 750 μl of full growth medium, incubated for 24 has described previously, and then treated with Zn-Pheide (7.5×10^{-7} M) for 2 h (37 °C, 5% CO_2). Images of Zn-Pheide fluorescence within cells were collected in the 657—679 nm range using excitation at 405 nm (diode laser, output 30 mW). The nuclei were stained with Hoechst 33342 solution (4 μg/ml) for 30 min, the fluorescence was excited at 405 nm as above, and recorded between 465 and 486 nm. The Golgi apparatus and endoplasmic reticulum were stained using a BODIPY® FL solution (0.2 μg/ml) for 15 min; the fluorescence was excited at 488 nm from a 30 mW argon laser and the emission was recorded in the 508—529 nm range. For lysosome detection, the cells were incubated for 30 min with LysoTracker® Yellow-HCK-123 solution (1.3 μg/ml) in PBS. The emission was measured between 529 and 550 nm, using a 458 nm excitation light from a 30 mW argon laser. In order to detect mitochondria, cells were incubated for 30 min with 10 nM tetramethylrhodamine methyl ester (TMRM), a cationic fluorescent derivative of Rhodamine 123 that is readily sequestered by active mitochondria. The TMRM emission was measured between 605 and 702 nm, using 543 nm excitation light. All images were recorded at 37 °C.

Cytotoxicity

Cell clonogenicity tests were performed with untreated cells only. Cell suspension was diluted to a density of 100 cells/ml in a cell growth medium and cells were cultured for 8 days. The clones were fixed, treated with Giemsa dye and counted. However, cells illuminated in the presence of the photosensitizer appeared too sensitive to trypsinization [24], and this made the clonogenic test unfeasible. For the MTT tests, the cells numbering 15×10^3 in 200 μl

Please cite this article in press as: Jakubowska M, et al. Zinc-pheophorbide *a*—Highly efficient low-cost photosensitizer against human adenocarcinoma in cellular and animal models. Photodiagnosis and Photodynamic Therapy (2013), http://dx.doi.org/10.1016/j.pdpdt.2012.12.004

of full growth medium were seeded in triplicates on 96-well plates and incubated overnight. A series of Zn-Pheide solutions (1×10^{-7} to 2×10^{-6} M) were prepared as described above and applied to the cells for 4, 24 and 48 h (37 °C, 5% CO_2) in the dark. After incubation, the cells were rinsed with PBS (200 μl) and then treated with 100 μl of MTT solution (0.5 g/l in 90% FCS-free growth medium) for 2.5 h. After MTT was reduced to violet formazan, the supernatant was removed and the formazan was dissolved in 100 μl of a methanol—DMSO mixture (1:1, v/v). The absorbance was measured at 560 nm. The calibration curves were prepared for each cell line individually, by measuring the amounts of reduced MTT absorbance as a function of cell number (not shown). To improve the accuracy of the readouts, a partial linear approximation of the standard curves was used. In the PDT experiments, the numbers of cells in each well were calculated from the respective absorbances, using the appropriate standard curve. The SF values were estimated as the ratios of the numbers of the treated and control cells. Control cells were incubated with the growth medium without FCS. The dark cytotoxicity experiments were repeated three times.

Cell death analysis

The A549 cells (5×10^3) in 200 μl of full growth medium (DMEM, high glucose, 10% FCS) were seeded in quadruplicates on 96-well Plates 24 h before the experiment. The cells were incubated with three different photosensitizers, Zn-Pheide, Chlide and Photofrin, each at 2×10^{-6} M, for 24 h in the dark. The cells were washed in PBS and irradiated with red light (7.98 J/cm^2). After the irradiation, PBS was replaced by the growth medium and cells were incubated for up to 24 h. In order to determine the cell death mechanisms, Hoechst 33342 (10 μg/ml, 30 min) and propidium iodide (PI, 45 μM, 15 min) were added. PI stains the nuclei of necrotic cells [25]. Hoechst 33342 stains viable and apoptotic nuclei [25]. The necrotic cells were identified by nuclear staining with PI with normal nuclear morphology while the viable cells and apoptotic cells were identified by staining with Hoechst 33342, and differentiated by nuclear morphology, i.e. the presence of apoptotic bodies. The total number of viable, necrotic, apoptotic and PI stained cells were counted per high power field per well [26,27]. The experiment was repeated three times and the results were calculated as mean values from three wells.

Photodynamic treatment

Light source. The cells were illuminated with an OSH150 illuminator equipped with a cut-off filter (>600 nm). The light intensity was determined between 500 and 850 nm and only the part of the source emission spectrum which overlaps with the absorption spectrum of Zn-Pheide was considered for the estimation of the absorbed dose *via* convolution procedure.

Light dose. The cells were seeded in triplicate as described above, and after a 2-h incubation with 5×10^{-7} M Zn-Pheide, cells were illuminated with red light (1.9×10^{-2} W/cm^2) for varying times of 0.5, 1.0, 2.5, 5.0, 10.0 and 15.0 min. The corresponding absorbed doses were estimated as 0.57, 1.14, 2.85, 5.7, 10.14 and 17.1 J/cm^2, respectively. The MTT viability test was carried out 48 h after the light treatment. The fraction of surviving cells was estimated as described above. The experiments were repeated five times.

Photosensitizer concentration. The cells (seeded in hexaplicates) and photosensitizer solutions (1×10^{-7} to 2×10^{-6} M) were prepared as described above. Cells were treated with Zn-Pheide for 2 h, rinsed with 200 μl PBS and then covered with a 200 μl portion of PBS. The illumination (5 min) was done using a red light intensity of 1.9×10^{-2} W/cm^2, to achieve an absorbed light dose equal to 5.7 J/cm^2. After the irradiation, cells were rinsed with PBS, a 200 μl of full culture medium was added to each well and they were allowed to grow for 48 h before performing the MTT viability test as described above. The fraction of surviving cells was estimated as described above.

Photodynamic therapy of tumors

The animals, BALB/cA nude (C.Cg/AgBomTac-Foxn1^{nu}N20) mice, were 7—8 weeks old males obtained from Taconic, Denmark. The A549 lung adenocarcinoma cells (1×10^6) were implanted subcutaneously into the left flanks of the animals. Tumors were palpable within 3—5 weeks after implantation and their three perpendicular diameters *a*, *b* and *c* were measured every 7 days, and their volumes were estimated as $(a \times b \times c)\pi/6$. When tumor volume reached approximately 110 mm^3, Zn-Pheide was administered to animals either i.p. at a dose of 10 mg/kg (3 animals) or i.v. at 1 mg/kg (7 animals). The solutions of the photosensitizer were prepared immediately before administration, by dissolving them in a small volume of EtOH and then adding PBS, or *aqua pro injectione* containing PBS (9/1). Before irradiation, the animals were anaesthetized using 8 mg/kg ketamine (Bioketan, Vetoquinol Biowet, Poland) and 30 mg/kg xylazine (Sedazin, Biowet, Poland) and their bodies were shielded from light, leaving only the tumor surface exposed. As a light source a 655 nm diode laser (Eurotek, Poland) was used, with a fluency of 100 mW/cm^2. The irradiation was performed 20 min (i.p.) or 70 min (i.v.) after the photosensitizer injection. The light dose was 120 J/cm^2 (20 min irradiation). The growth of tumors was monitored for up to 120 days after PDT. Nine untreated animals bearing the same tumors served as control. All experimental procedures were approved by Local Ethical Committee for Animal Experimentation in Kraków (decision no. 14/2011).

Histological analysis

One hundred and twenty days after the treatment, the animals were sacrificed and the tumors excised for histological analysis. Formaldehyde fixed and paraffin embedded tumor slides (5 μm) were stained with hematoxylin and eosin. The slides were then inspected under a light microscope and photographed.

Statistical analysis

All statistical analyses were performed using Student's *t*-test. A *p* value below 0.05 was considered significant.

Please cite this article in press as: Jakubowska M, et al. Zinc-pheophorbide *a*—Highly efficient low-cost photosensitizer against human adenocarcinoma in cellular and animal models. Photodiagnosis and Photodynamic Therapy (2013), http://dx.doi.org/10.1016/j.pdpdt.2012.12.004

Results

Cellular uptake and localization of Zn-Pheide

The A549, MCF-7 and LoVo cells were incubated (2, 6, 12 and 24 h) in Zn-Pheide solutions at concentrations ranging from 1×10^{-7} to 5×10^{-7} M and its intracellular levels were estimated by a fluorometric analysis of acetone extracts of the cells. The results of this analysis are shown in Fig. S1. There is almost no uptake (emission intensity near the background) of Zn-Pheide when applied at the lowest concentration. At two higher concentrations, 2×10^{-7} and 5×10^{-7} M, the cellular level of Zn-Pheide kept increasing for up to 12 h of incubation in all three cell lines, and then decreased (Fig. S1).

The relationship between the concentration of Zn-Pheide in the incubation medium and its intracellular level is linear (Table S1, Supplementary data) and the accumulation factor ranges between 18 and 25, approaching the values estimated for other porphyrinic pigments [28,29]. This suggests that Zn-Pheide has a strong affinity to the cells and there is a very preferential partition of the pigment between the aqueous medium and the cellular interior.

To determine the intracellular localization of Zn-Pheide, the A549, MCF-7 and LoVo cells were loaded with both the photosensitizer (7.5×10^{-7} M, 2 h) and the organelle-selective fluorescent probes. The cells were treated with Hoechst 33342 in order to label the nuclei (Fig. 2C and I), with BODIPY® FL to label the system of intracellular membranes (endoplasmic reticulum, ER) and the Golgi apparatus (Fig. 2E and K) and with LysoTracker Yellow-HCK-123 to stain the lysosomes (Fig. 2F). The results were analyzed by means of laser confocal microscopy (Fig. 2) and a combination of appropriate probes and narrow-pass filters enabled a precise determination of sites for the subcellular accumulation of Zn-Pheide. A comparison of the confocal images shows that emission of Zn-Pheide fluorescence coincides both with cell compartments labeled with BODIPY® FL (compare Fig. 2D and E) and with LysoTracker-HCK-123 (compare Fig. 2D and F) while its emission is undetectable in the nuclei. Interestingly, in contrast to most chlorophyllide derivatives [30—33], no localization of Zn-Pheide was found in the mitochondria stained with TMRM as the marker (Fig. 2M). This result was confirmed using Rhodamine123 as a mitochondrial marker in a different tumor cell line (Fig. S2). This is in line with an earlier report showing another pheophorbide *a* derivative that does not penetrate into the mitochondria [34]. All these results clearly indicate that the system of intracellular membranes and lysosomes are the preferred sites of Zn-Pheide accumulation.

Dark cytotoxicity of Zn-Pheide

The dark toxicity of Zn-Pheide was tested after 4, 24 and 48 h incubations. Zn-Pheide had no effect on the viability of the cells up to a concentration of 2×10^{-6} M for 4 h incubation time (Fig. S3A). For 24 and 48 h incubations, the viability of MCF-7 cells in 1×10^{-6} M and 2×10^{-6} M of Zn-Pheide decreased to 80% and 50%, respectively (Fig. S3B and C). This indicates that the dark cytotoxicity of Zn-Pheide at the concentrations used in photodynamic experiments, up to 2×10^{-6} M, is low.

Cellular responses to photodynamic treatment

In an attempt to estimate the cell surviving fraction (SF) following photodynamic treatment with Zn-Pheide, clonogenicity tests were performed (not shown). The untreated cells showed a good clonogenic efficacy (A549: 48%, MCF-7: 81%, LoVo: 70%), although, upon illumination in the presence of the photosensitizer, the cells appeared to be too sensitive to trypsinization which considerably lowered the accuracy of the test [24]. Therefore, the MTT-based method was chosen as more reliable in the analysis of the SF after photodynamic treatment. In order to assess the photodynamic effect on the cell lines in function of light dose or photosensitizer concentration, the cells were exposed for 2 h to Zn-Pheide at 5×10^{-7} M, and then illuminated with red light ($\lambda > 600$ nm, Fig. 1), the light doses applied varied from 0 to 17 J/cm^2. The dependence of SF on the light dose is shown in Fig. 3A. The drop in SF was very steep even at low light doses and the three cell lines showed some differences in their response, with the A549 cells being most sensitive, reaching a 100% mortality already at 5.7 J/cm^2. However, a complete elimination of the MCF-7 and LoVo cells could not be achieved, even with the highest light doses, because a fraction of about 10% of the cells always remained alive. The differences between the three model cell lines in their cellular responses are even more pronounced in the dependence of the SF on photosensitizer concentration (Fig. 3B). Again, the A549 cells were the most sensitive, the SF for MCF-7 decreased to zero at 1×10^{-6} M, and a 10% fraction of LoVo remained alive, even with the highest concentration of Zn-Pheide (2×10^{-6} M).

Comparison to other photosenstizers

The photodynamic properties of Zn-Pheide were compared to those of Photofrin and Chlide in a cellular model using the A549 line. The cells were treated with each photosensitizer at the same concentration (1.4 μg/ml, corresponding to $\sim 2 \times 10^{-6}$ M; no dark toxicity), 24 h afterwards irradiated with red light (7.98 J/cm^2), and the cell death mechanisms were investigated. The cells were monitored after 6, 12 and 24 h following the treatment and classified as alive, apoptotic, necrotic and PI-positive (Fig. 4, Supplementary Table S2). No living cells remained in the culture treated with either Chlide or Zn-Pheide, whereas as many as almost 90% of cells treated with Photofrin were found alive after 24 h. As seen in Fig. 4 and Table S2, a substantial degree of apoptosis was observed in the case of the Chla derivatives. Zn-Pheide caused a slightly higher (17%) fraction of PI-positive cells than Chlide, suggesting faster cell death in this case.

Photofrin is known to induce apoptosis, both *in vitro* and *in vivo*, but requires much higher concentrations [35,36]. For instance, after a 6 h treatment with this drug at 30 μg/ml with light at 6 J/cm^2, up to 50% apoptosis was seen in the A549 cells [37]. Our results obtained at a slightly higher light dose (8 J/cm^2) show a similar level of apoptosis in these cells with as little as 1.4 μg/ml of Zn-Pheide, i.e. a 20-fold lower concentration. This confirms the very high

Please cite this article in press as: Jakubowska M, et al. Zinc-pheophorbide *a*—Highly efficient low-cost photosensitizer against human adenocarcinoma in cellular and animal models. Photodiagnosis and Photodynamic Therapy (2013), http://dx.doi.org/10.1016/j.pdpdt.2012.12.004

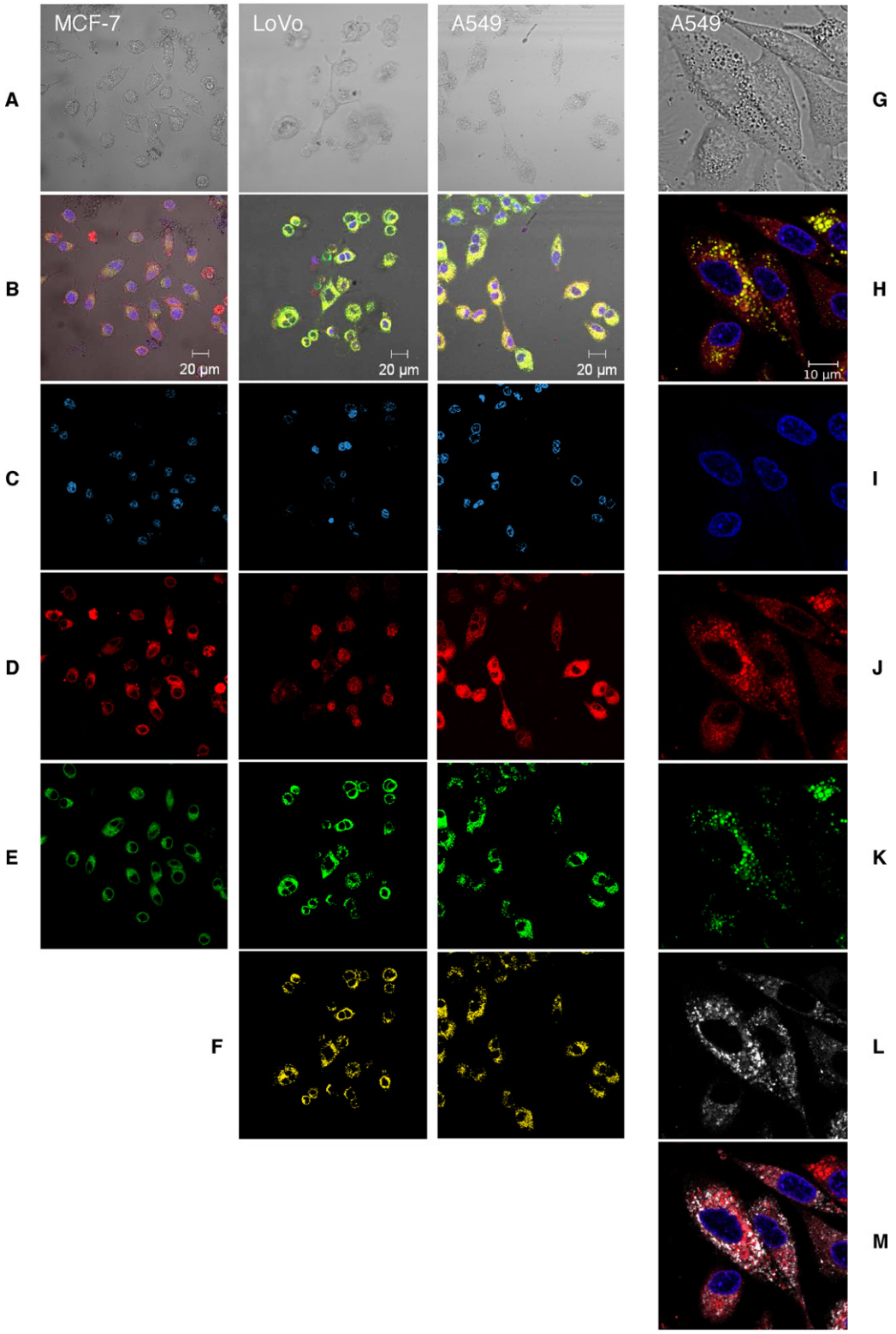

Figure 2 Confocal images of the A549, MCF-7 and LoVo cells, showing the localization of Zn-Pheide and organelle-selective fluorescent probes (A—F, scale bar: 20 μm) and A549 cells (G—M, scale bar: 10 μm). (A and G) Differential interference contrast (DIC) images. (B) Overlay of laser confocal images C—F, demonstrating Zn-Pheide localization in system of intracellular membranes and lysosomes. (C and I) Cells stained with Hoechst 33342. (D and J) Cells treated with Zn-Pheide. (E and K) Cells stained with BODIPY FL. (F) Cells stained with LysoTracer Yellow-HCK-123 (the MCF-7 cells could not be stained for lysosomal detection). (H) Overlay of images I—K, demonstrating Zn-Pheide localization in system of intracellular membranes. (L) A549 cells stained with TMRM, the mitochondria marker. (M) Overlay of I, J and L showing the absence of Zn-Pheide localization in mitochondria.

Please cite this article in press as: Jakubowska M, et al. Zinc-pheophorbide *a*—Highly efficient low-cost photosensitizer against human adenocarcinoma in cellular and animal models. Photodiagnosis and Photodynamic Therapy (2013), http://dx.doi.org/10.1016/j.pdpdt.2012.12.004

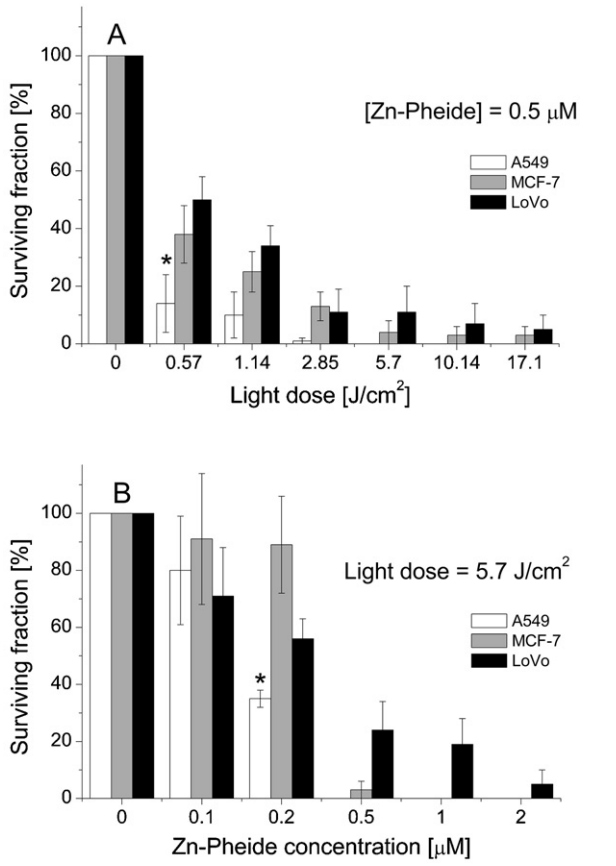

Figure 3 Survival of the adenocarcinoma cells following the photodynamic treatment with Zn-Pheide. The effect of light dose (A) and of Zn-Pheide concentration (B) on SF of the A549 (white), MCF-7 (gray) and LoVo cells (black). Cell viability was assessed by the MTT reduction assay, carried out 48 h after the photodynamic treatment (see the text for details). The results are represented as means ± SE for $N = 5$, $n = 15$ (A), and $N = 3$, $n = 18$ (B). The star shows statistically significant difference between cell lines for a given light or PS dose.

phototoxicity of this photosensitizer. Such a substantial discrepancy in the photodynamic effects caused by Photofrin and Zn-Pheide cannot be explained merely on the basis of any large difference in their extinction coefficient in the red part of the spectrum. In terms of the energies absorbed effectively by the photosensitizers under the conditions of the *in vitro* study an estimation done *via* a comparison of the overlaps of the absorption spectra with the source spectrum (Fig. 1) yielded a factor of only four.

In vivo study

In the *in vivo* study, 10 animals (BALB/cA nude mice) bearing A549 tumor were treated with Zn-Pheide and light, and several different PDT protocols were evaluated beforehand (not shown). Zn-Pheide doses were tested in the range between 1—10 mg/kg for i.p. injections and 1—2 mg/kg for i.v., based on the pharmacokinetics study [19]. The prodrug-light intervals from 0 to 300 min were applied. The photosensitizer doses were chosen on the basis of the most effective protocols: in one Zn-Pheide was administered i.v. at a dose of 1 mg/kg and in the other the photosensitizer was administered i.p. at 10 mg/kg. In the former protocol, the dose is limited by the solubility of the photosensitizer and the volume (~0.2 ml) that can be i.v. administered. Therefore, in order to check the dose-therapeutic effect relationship, the i.p. method was applied too.

The growth of tumors and general state of the animals were monitored for four months after the therapy; the animals were sacrificed when the control tumors reached 10% of body weight and the tumors were excised for histological analysis. Untreated tumors ($n = 9$) demonstrated a biphasic growth, with a pronounced acceleration from the 10th week on, reaching a plateau near the week 15. Only a weak tumor swelling effect was observed shortly after the PDT, in contrast to treatment based on other photosensitizers which cause a long term edema [38,39]. Moreover, neither skin phototoxicity nor changes in animal behavior were observed, and all the animals which underwent the treatment were in good general health.

Structures characteristic of adenocarcinoma and only focal areas of necrosis were found in untreated tumors, as shown in Fig. 5. The tumors had well developed vasculature and formed solid areas of proliferating cells with hyperchromatic nuclei and adenoid structures. The PDT treatment induced extensive necrosis in the tumors (Fig. 5) and completely inhibited their growth (Fig. 6). A histological examination showed that only a few viable cells and infiltrating leukocytes were visible (Fig. 5C and D). Most importantly, the tumor size on average was reduced 5-fold

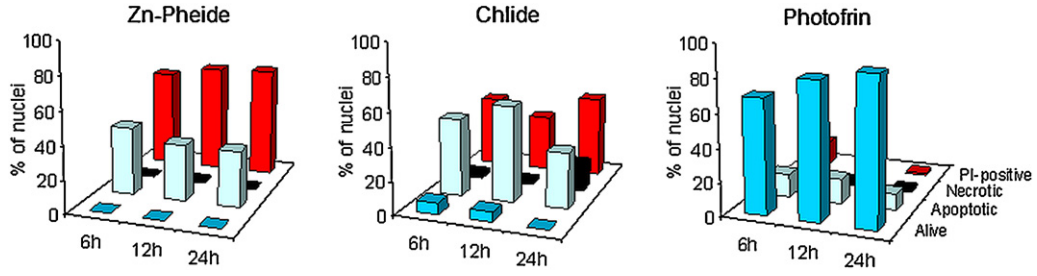

Figure 4 Percentage of A549 cells classified as alive, apoptotic, necrotic and PI-positive, following the photodynamic treatment with Zn-Pheide, Chlide and Photofrin. The same concentration of PS was used: 1.4 μg/ml. 24 h after, 7.98 J/cm² of red light was applied. The results as represented as means for $N = 3$, $n = 9$. A detailed statistical analysis is shown in Table S2 (Supplementary materials).

Please cite this article in press as: Jakubowska M, et al. Zinc-pheophorbide *a*—Highly efficient low-cost photosensitizer against human adenocarcinoma in cellular and animal models. Photodiagnosis and Photodynamic Therapy (2013), http://dx.doi.org/10.1016/j.pdpdt.2012.12.004

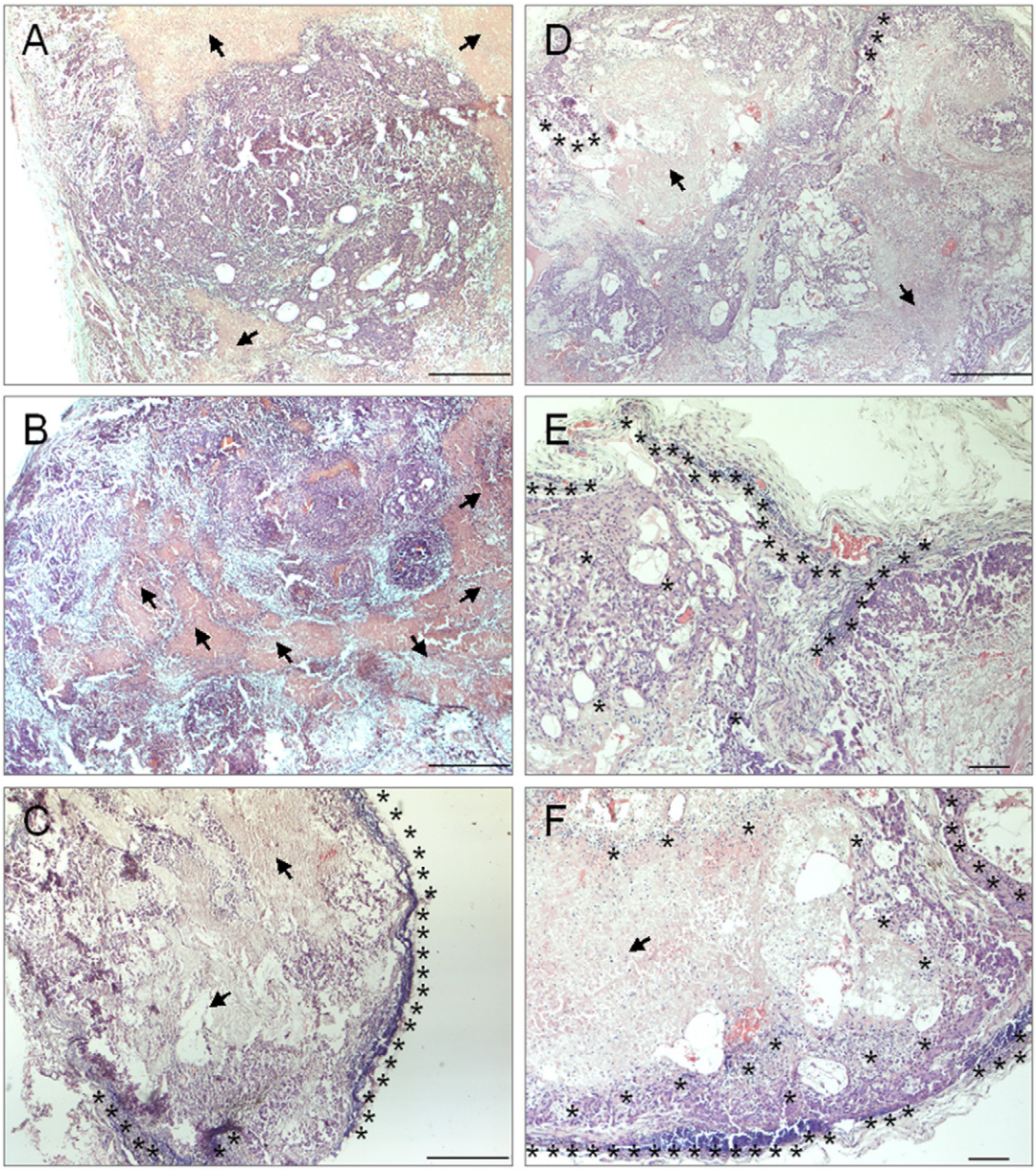

Figure 5 Photomicrographs of hematoxylin and eosin stained paraffin sections of the A549 human lung adenocarcinoma tumors transplanted into the BALB/cA nude mice, taken without and after PDT with Zn-Pheide. (A and B) Sections of controls, magnification 40×, scale bar 500 μm; (C and D) sections of tumors following PDT, magnification 40×, scale bar 500 μm; (E and F) sections of tumor following PDT, magnification 100×, scale bar 100 μm. (D—F) Massive necrosis in tumors after PDT, using Zn-Pheide i.p. at 10 mg/kg (C) and i.v. at 1 mg/kg, with complete obliteration of the tumor tissue. Infiltrating leukocytes indicated with asterisks, necrotic areas indicated with arrows. (A, B) Sections of two different control (untreated) tumors, (C) a PDT-subjected tumor, (D-F) sections of PDT-subjected tumor, different than in C.

in comparison to the control. Individually, tumors treated with Zn-Pheide and light either regressed (30% success, in 3 out of 10 cases), displayed growth inhibition (in 6 out of 10 cases), or did not changed (in 1 out of 10 cases). In the best instance, the tumor was almost eliminated (the volume reduced 80-fold!). Both the outcome of histological analysis (Fig. 5) and the kinetics of the tumor growth (Fig. 6) clearly demonstrate that indeed Zn-Pheide-based PDT leads to an almost complete eradication of the tumor tissue.

Discussion

Photosensitizer localization

The subcellular localization of a photosensitizer (or any xenobiotic) is obviously determined by its chemical structure and its specific and non-specific interactions with the environment. For intact Chls (Fig. 1), the main determinants of their interactions with the environment and their

Please cite this article in press as: Jakubowska M, et al. Zinc-pheophorbide *a*—Highly efficient low-cost photosensitizer against human adenocarcinoma in cellular and animal models. Photodiagnosis and Photodynamic Therapy (2013), http://dx.doi.org/10.1016/j.pdpdt.2012.12.004

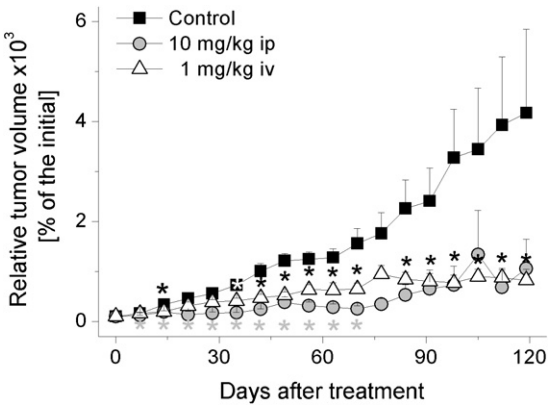

Figure 6 A significant inhibition of A549 tumor growth in mice after PDT with Zn-Pheide up to 120 days. Tumor growth is presented as the tumor volume relative to its volume at the day of treatment. The initial tumor mean diameters varied from 4 to 8 mm. The photosensitizer was administrated either i.p. at 10 mg/kg (gray circles) or i.v. at 1 mg/kg (open triangles). Asterisks indicate significant differences in tumor growth ($p < 0.05$) after PDT using i.p. ($n = 3$) and i.v. ($n = 7$) injection, respectively. Untreated animals (black squares) are control ($n = 9$). The results are represented as means ± SD.

binding to photosynthetic proteins are the phytyl chain, a set of conservative peripheral groups, and the central Mg^{2+} ion [40]. In the case of Zn-Pheide, the coordination of axial ligands to the central metal seems to be of little relevance because the Zn^{2+} ion in such complexes only weakly binds one axial ligand [13]. Thus, in chlorophyllides, the absence of a very hydrophobic phytyl chain and the presence of a free carboxylic group are the major factors which increase their solubility in aqueous media [8,19]. The distribution of chlorophyllides in biological membranes may then be charge/pH-sensitive. In regions of higher pH, the interactions of the deprotonated carboxyl group with positively charged lipids will be favored, resulting in their affinity to those membrane compartments which are rich in such lipids [41,42]. Because the localization of Zn-Pheide is quite similar to that of simple porphyrins, e.g. protoporphyrin IX or hematoporphyrin derivative [43,44], the interactions with other peripheral groups seem to be of lesser significance in determining the cellular location. Seemingly, the general structural motifs common to both types of photosensitizers, i.e. the tetrapyrrolic macrocycle with a system of delocalized π-electrons and carboxylic group(s), are the major determinants of their cellular localization.

The localization of Zn-Pheide in the Golgi apparatus and ER, i.e. in a hydrophobic environment, seems favorable for therapeutic purposes. On the one hand, aggregation of the photosensitizer is less likely to occur in a non-polar environment [45], and, on the other, the lifetime of singlet oxygen is prolonged in such media [46]. Moreover, photodynamic action induced directly in ER may more effectively contribute to oxidative stress [47,48], leading to major changes in ER function, e.g. a release of Ca^{2+} and the aggregation of unfolded and misfolded proteins [49]. Similarly, the lysosomal accumulation is expected to enhance photodamage due to the release of hydrolases [45]. It remains unclear at the moment, why Zn-Pheide shows no accumulation in mitochondria.

Photodynamic effect on cells

In spite of the very similar intracellular localizations and levels of Zn-Pheide, there are differences between human adenocarcinoma cells in the response to photodynamic treatment. The A549 cells are the most sensitive, while the elimination of MCF-7 and LoVo cells requires higher doses of photosensitizer and/or light. These differences could not be attributed to rather non-significant differences in Zn-Pheide uptake at the 2 h incubation time (Fig. S1). Several factors might be responsible for these differences in cell viability, and at present, without a more detailed study, it is only possible to suggest the most plausible ones. One of them might be the activity of the cellular defense system, which involves the mobilization of a variety of ROS-quenching mechanisms and these can vary in different cell lines, e.g. the thiol content [50—52]. Some authors point to another factor, a physical one, which may determine the degree of cellular response to the photodynamic effect, which is the inhomogeneous distribution of molecular oxygen in microregions within the cell. The differences in oxygen concentration between intra- and extracellular compartments, in spite of the same oxygenation level in the cell culture have been documented [53,54]. For instance, the differences in metabolic rates between cell lines may lead to a different effective amount of intracellular and intra-membrane oxygen and limit the photodynamic effect.

Therapeutic efficacy

(B)Chl-based and other structurally similar photosensitizers have already been applied with success in PDT, including experimental tumors, animal and human xenografts [1,55]. For instance, Talaporfin at 10 mg/kg with light dose of 100 J/cm^2 at 100 mW/cm^2 eradicated Meth-A fibrosarcoma tumors within 90 days [56]. A treatment of Colo26 tumors using Photochlor (HPPH) at 0.3 mg/kg with light dose of 128/cm^2 at 14 mW/cm^2 resulted in tumor control for 80 days [32]. The growth of resistant mouse melanoma tumors was inhibited for up to two months using a halogenated bacteriochlorin as the photosensitizer at 10 mg/kg and 108 J/cm^2 of 750 nm light [57]. Tookad, a vascular-targeting agent, was very effective against melanoma tumors, where a dose of 9 mg/kg and 30 J/cm^2 led to tumor cure in 70% of cases for 90 days [58]. In human xenografts, slightly higher doses of the drug and/or light had to be used [31]. In the present study, Zn-Pheide at 1 mg/kg and 120 J/cm^2 brought about a complete control of human adenocarcinoma tumors, lasting up to 4 months. Besides this high tumor control efficiency, the advantage of Zn-Pheide based PDT lies also in the fact that absolutely no skin damage was observed after PDT, which is a frequently seen side effect of PDT. Our results demonstrate that Zn-Pheide is an efficient photosensitizer, particularly useful for targeting tumor cancer cells. Interestingly, both PDT protocols, which differ by one order of magnitude in the drug dose, yielded similar results, and therefore a dose of 1 mg/kg, of Zn-Pheide administered i.v., fully suffices to achieve a strong therapeutic effect. On the other hand,

Please cite this article in press as: Jakubowska M, et al. Zinc-pheophorbide *a*—Highly efficient low-cost photosensitizer against human adenocarcinoma in cellular and animal models. Photodiagnosis and Photodynamic Therapy (2013), http://dx.doi.org/10.1016/j.pdpdt.2012.12.004

an intriguing question remains as to why a 10 times higher dose of the photosensitizer causes a very similar therapeutic response. This will be the subject of another study.

Conclusions

A complete inhibition of the tumor with no regrowth for up to 4 months was observed following the application of Zn-Pheide as a photosensitizer in the PDT of human adenocarcinoma in an animal model. In parallel, the *in vitro* study shows that Zn-Pheide is quickly taken up by cells and localizes mainly in the intracellular membranes and vesicles. In contrast to most derivatives of chlorophyll *a*, Zn-Pheide does not localize to mitochondria. A strong photodynamic effect can be achieved even with extremely low doses of the photosensitizer (5×10^{-7} M) and fairly low light doses (around 5—8 J/cm^2). These results demonstrate several advantageous features of Zn-Pheide as a promising photosensitizer. Namely, the excellent light-absorption properties, a low dark cytotoxicity, and a very high photocytotoxicity against tumor *in vivo*, resulting in the inhibition or even a regression of human lung cancer xenografts in nude mice after a single treatment. In addition, the known pharmacokinetics of Zn-Pheide together with its semi-synthetic origin, availability and ease of synthesis resulting in high cost-efficiency underlie its value as a very promising photosensitizing agent for PDT.

Acknowledgments

The authors would like to thank Dr. J. Saczko (Department of Medical Biochemistry, Wroclaw Medical University, Wroclaw, Poland) for the generous gift of the adenocarcinoma cell lines, and Dr. D. Nowis (Department of Immunology, Medical University of Warsaw, Warsaw, Poland) for the Photofrin. The Laboratory of Confocal Imaging (Department of Cytology and Histology, Institute of Zoology, Jagiellonian University) is acknowledged for providing access to the confocal microscope (LSM 510 META, Axiovert 200M, ConfoCor 3, Carl Zeiss MicroImaging GmbH, Jena, Germany), and P. Weber and W. Krzeptowski are thankfully acknowledged for their assistance with confocal imaging. We also thank Laboratory of Cell Biophysics for use of Leica SMD confocal microscope and E. Biela for assistance. A. Bartelik, veterinarian, is gratefully acknowledged for the animal care. The work was supported by grants from the Polish Ministry of Science and Higher Education (R05 043 03 to K.U., and 0519/B/P01/2011/40 to L.F.), National Science Center (0505/B/P01/2011/40 to K.U.), The Foundation for Polish Science (TEAM/2010-5/3 to L.F.), and a stipend to M.J., provided by the Malopolska Region. The Faculty of Biochemistry, Biophysics and Biotechnology of the Jagiellonian University is beneficiary of structural funds from the European Union (grant no: POIG.02.01.00-12-064/08 — *Molecular biotechnology for health*).

Appendix A. Supplementary data

Supplementary data associated with this article can be found, in the online version, at http://dx.doi.org/10.1016/j.pdpdt.2012.12.004.

References

[1] Brandis A, Salomon Y, Scherz A. Chlorophyll sensitizers in photodynamic therapy. In: Grimm B, Porra R, Rudiger W, Scheer H, editors. Chlorophylls and bacteriochlorophyls: biochemistry, biophysics, functions and applications. Dordrecht: Springer; 2006. p. 462—83.

[2] Juarranz A, Jaen P, Sanz-Rodriguez F, Cuevas J, Gonzalez S. Photodynamic therapy of cancer, basic principles and applications. Clinical and Translational Oncology 2008;10:148—54.

[3] Yano S, Hirohara S, Obata M, Hagiya Y, Ogura S-i, Ikeda A, et al. Current states and future views in photodynamic therapy. Journal of Photochemistry and Photobiology C: Photochemistry Reviews 2011;12:46—67.

[4] Agostinis P, Berg K, Cengel KA, Foster TH, Girotti AW, Gollnick SO, et al. Photodynamic therapy of cancer: an update. CA: A Cancer Journal for Clinicians 2011;61:250—81.

[5] Hasan TB, Ortel B, Moor ACE, Pogue BW. Photodynamic therapy of cancer. In: Kufe DW, Pollock RE, Weichselbaum RR, Bast RC, Gansler TS, Holland JF, Frei E, editors. Holland-Frei cancer medicine. Hamilton: Decker Publishing Inc.; 2003. p. 605—22.

[6] Pandey RK, Goswami LN, Chen Y, Gryshuk A, Missert JR, Oseroff A, et al. Nature: a rich source for developing multifunctional agents. Tumor-imaging and photodynamic therapy. Lasers in Surgery and Medicine 2006;38:445—67.

[7] Preise D, Scherz A, Salomon Y. Antitumor immunity promoted by vascular occluding therapy: lessons from vascular-targeted photodynamic therapy (VTP). Photochemistry and Photobiology Science 2011;10:681—8.

[8] Fiedor L, Gorman A, Hamblett I, Rosenbach-Belkin V, Salomon Y, Scherz A, et al. A pulsed laser and pulse radiolysis study of amphiphilic chlorophyll derivatives with PDT activity toward malignant melanoma. Photochemistry and Photobiology 1993;58:506—11.

[9] Fiedor J, Fiedor L, Winkler J, Scherz A, Scheer H. Photodynamics of the bacteriochlorophyll-carotenoid system 1. Bacteriochlorophyll-photosensitized oxygenation of b-carotene in acetone. Photochemistry and Photobiology 2001;74:64—71.

[10] Spikes JD, Bommer JC. Chlorophyll and related pigments as photosensitizers in biology and medicine. In: Scheer H, editor. Chlorophylls. Boca Raton: CRC Press; 1991. p. 1181—204.

[11] Henderson BW, Sumlin AB, Owczarczak BL, Dougherty TJ. Bacteriochlorophyll-a as photosensitizer for photodynamic treatment of transplantable murine tumors. Journal of Photochemistry and Photobiology 1991;10:303—13.

[12] Fiedor L, Rosenbach-Belkin V, Sai M, Scherz A. Preparation of tetrapyrole—amino acid covalent complex. Plant Physiology and Biochemistry 1996;34:393—8.

[13] Hartwich G, Fiedor L, Simonin I, Cmiel E, Schäfer W, Noy D, et al. Metal-Substituted Bacteriochlorophylls 1. Preparation and Influence of Metal and Coordination on Spectra. Journal of the American Chemical Society 1998;120:3675—83.

[14] Drzewiecka-Matuszek A, Skalna A, Karocki A, Stochel G, Fiedor L. Effects of heavy central metal on the ground and excited states of chlorophyll. Journal of Biological Inorganic Chemistry 2005;10:453—62.

[15] Koudinova NV, Pinthus JH, Brandis A, Brenner O, Bendel P, Ramon J, et al. Photodynamic therapy with Pd-bacteriopheophorbide (Tookad): successful in vivo treatment of human prostatic small cell carcinoma xenographs. International Journal of Cancer 2003;104:782—9.

[16] Weersink RA, Bogaards A, Gertner M, Davidson SR, Zhang K, Netchev G, et al. Techniques for delivery and monitoring of TOOKAD (WST09)-mediated photodynamic therapy of the prostate: clinical experience and practicalities. Journal of Photochemistry and Photobiology B 2005;79:211—22.

Please cite this article in press as: Jakubowska M, et al. Zinc-pheophorbide *a*—Highly efficient low-cost photosensitizer against human adenocarcinoma in cellular and animal models. Photodiagnosis and Photodynamic Therapy (2013), http://dx.doi.org/10.1016/j.pdpdt.2012.12.004

[17] Davidson SR, Weersink RA, Haider MA, Gertner MR, Bogaards A, Giewercer D, et al. Treatment planning and dose analysis for interstitial photodynamic therapy of prostate cancer. Physics in Medicine and Biology 2009;54:2293—313.
[18] Berdugo M, Bejjani RA, Valamanesh F, Savoldelli M, Jeanny JC, Blanc D, et al. Evaluation of the new photosensitizer Stakel (WST-11) for photodynamic choroidal vessel occlusion in rabbit and rat eyes. Investigative Ophthalmology and Visual Science 2008;49:1633—44.
[19] Szczygiel M, Urbanska K, Jurecka P, Stawoska I, Stochel G, Fiedor L. Central metal determines pharmacokinetics of chlorophyll-derived xenobiotics. Journal of Medicinal Chemistry 2008;51:4412—8.
[20] Doyle LA, Ross DD. Multidrug resistance mediated by the breast cancer resistance protein BCRP (ABCG2). Oncogene 2003;22:7340—58.
[21] Szakacs G, Paterson JK, Ludwig JA, Booth-Genthe C, Gottesman MM. Targeting multidrug resistance in cancer. Nature Drug Discovery 2006;5:219—34.
[22] Fiedor L, Rosenbach-Belkin V, Scherz A. The stereospecific interaction between chlorophylls and chlorophyllase, possible implication for chlorophyll biosynthesis and degradation. Journal of Biological Chemistry 1992;267:22043—7.
[23] Detty MR, Gibson SL, Wagner SJ. Current clinical and preclinical photosensitizers for use in photodynamic therapy. Journal of Medicinal Chemistry 2004;47:3897—915.
[24] Ball DJ, Mayhew S, Vernon DI, Griffin M, Brown SB. Decreased efficiency of trypsinization of cells following photodynamic therapy: evaluation of a role for tissue transglutaminase. Photochemistry and Photobiology 2001;73:47—53.
[25] Crissman H. Cell cycle analysis by flow cytometry. In: Studzinski G, editor. Cell growth and apoptosis. Oxford: IRL Press; 1995. p. 21—43.
[26] Wyld L, Reed MW, Brown NJ. Differential cell death response to photodynamic therapy is dependent on dose and cell type. British Journal of Cancer 2001;84:1384—6.
[27] Eguchi Y, Shimizu S, Tsujimoto Y. Intracellular ATP levels determine cell death fate by apoptosis or necrosis. Cancer Research 1997;57:1835—40.
[28] Woodburn KW, Vardaxis NJ, Hill JS, Kaye AH, Reiss JA, Phillips DR. Evaluation of porphyrin characteristics required for photodynamic therapy. Photochemistry and Photobiology 1992;55:697—704.
[29] Rosenbach-Belkin V, Chen L, Fiedor L, Tregub I, Pavlotsky F, Brumfeld V, et al. Serine conjugates of chlorophyll and bacteriochlorophyll: photocytotoxicity and tissue distribution in mice bearing melanoma tumors. Photochemistry and Photobiology 1996;64:174—81.
[30] MacDonald IJ, Morgan J, Bellnier DA, Paszkiewicz GM, Whitaker JE, Litchfield DJ, et al. Subcellular localization patterns and their relationship to photodynamic activity of pyropheophorbide-a derivatives. Photochemistry and Photobiology 1999;70:789—97.
[31] Plaks V, Koudinova N, Nevo U, Pinthus JH, Kanety H, Eshhar Z, et al. Photodynamic therapy of established prostatic adenocarcinoma with TOOKAD: a biphasic apparent diffusion coefficient change as potential early MRI response marker. Neoplasia 2004;6:224—33.
[32] Henderson BW, Gollnick SO, Snyder JW, Busch TM, Kousis PC, Cheney RT, et al. Choice of oxygen-conserving treatment regimen determines the inflammatory response and outcome of photodynamic therapy of tumors. Cancer Research 2004;64:2120—6.
[33] Dougherty TJ. An update on photodynamic therapy applications. Journal of Clinical Laser Medicine and Surgery 2002;20:3—7.
[34] Matroule JY, Bonizzi G, Morliere P, Paillous N, Santus R, Bours V, et al. Pyropheophorbide-a methyl ester-mediated photosensitization activates transcription factor NF-kappaB through the interleukin-1 receptor-dependent signaling pathway. Journal of Biological Chemistry 1999;274:2988—3000.
[35] Berlanda J, Kiesslich T, Engelhardt V, Krammer B, Plaetzer K. Comparative in vitro study on the characteristics of different photosensitizers employed in PDT. Journal of Photochemistry and Photobiology B 2010;100:173—80.
[36] Nonaka T, Nanashima A, Nonaka M, Uehara M, Isomoto H, Asahina I, et al. Analysis of apoptotic effects induced by photodynamic therapy in a human biliary cancer cell line. Anticancer Research 2010;30:2113—8.
[37] Saczko J, Chwilkowska A, Kulbacka J, Berdowska I, Zielinski B, Drag-Zalesinska M, et al. Photooxidative action in cancer and normal cells induced by the use of photofrin in photodynamic therapy. Folia Biologica 2008;54:24—9.
[38] Li L, Luo R, Liao W, Zhang M, Luo Y, Miao J. Clinical study of photofrin photodynamic therapy for the treatment of relapse nasopharyngeal carcinoma. Photodiagnosis and Photodynamic Therapy 2006;3.
[39] Wyss P, Schwarz V, Dobler-Girdziunaite D, Hornung R, Walt H, Degen A, et al. Photodynamic therapy of locoregional breast cancer recurrences using a chlorin-type photosensitizer. International Journal of Cancer 2001;93:720—4.
[40] Fiedor L, Kania A, Mysliwa-Kurdziel B, Stochel G. Understanding chlorophylls: central magnesium and phytyl as structural determinants. Biochimica et Biophysica Acta 2008;1777:1491—500.
[41] Brault D. Physical chemistry of porphyrins and their interactions with membranes: the importance of pH. Journal of Photochemistry and Photobiology B 1990;6:79—86.
[42] Al-Omari S. Photophysical properties and localization of chlorins substitutes with metoxy groups, hydroxyl groups and alkyl chains in liposome-like cellular membrane. Biomedicine Materials 2007;2:107—15.
[43] Ji Z, Yang G, Vasovic V, Cunderlikova B, Suo Z, Nesland JM, et al. Subcellular localization pattern of protoporphyrin IX is an important determinant for its photodynamic efficiency of human carcinoma and normal cell lines. Journal of Photochemistry and Photobiology B: Biology 2006;84:213—20.
[44] Sun X, Leung W. Photodynamic therapy with pyropheophorbide-a methyl ester in human lung carcinoma cancer cell: efficacy, localization and apoptosis. Photochemistry and Photobiology 2002;75:644—51.
[45] Bonnet R. Chemical aspects of photodynamic therapy. Amsterdam: Gordon and Breach Science Publishers; 2000.
[46] Kohen E, Santus R, Hirschberg JG. Photobiology. San Diego: Academic Press; 1995.
[47] Mak N-K, Li K-M, Leung W-N, Wong R-S, Huang D, Lung M, et al. Involvement of both endoplasmic reticulum and mitochondria in photokilling of nasopharyngeal carcinoma cells by the photosensitizer Zn-BM-AM. Biochemical Pharmacology 2004;68:2387—96.
[48] Marchal S, Francois A, Dumas D, Guillemin F, Bezdetnaya L. Relationship between subcellular localization of Foscan® and caspase activation in photosensitized MCF-7 cells. British Journal of Cancer 2007;96:944—51.
[49] Oleinick NL, Nieminen AL, Chiu SM. Cell killing by photodynamic therapy. In: Hamblin MR, Mroz P, editors. Advances in photodynamic therapy. Norwood, MA, USA: Artech House; 2008. p. 115—33.
[50] Robaszkiewicz A, Balcerczyk A, Bartosz G. Antioxidative and prooxidative effects of quercetin on A549 cells. Cell Biology International 2007;31:1245—50.
[51] Shrivastava A, Tiwari M, Sinha RA, Kumar A, Balapure AK, Bajpai VK, et al. Molecular iodine induces caspase-independent apoptosis in human breast carcinoma cells involving the mitochondria-mediated pathway. Journal of Biological Chemistry 2006;281:19762—71.

Please cite this article in press as: Jakubowska M, et al. Zinc-pheophorbide *a*—Highly efficient low-cost photosensitizer against human adenocarcinoma in cellular and animal models. Photodiagnosis and Photodynamic Therapy (2013), http://dx.doi.org/10.1016/j.pdpdt.2012.12.004

[52] Watts ME, Dennis MF, Roberts IJ. Radiosensitization by misonidazole, pimonidazole and azomycin and intracellular uptake in human tumour cell lines. International Journal of Radiation Biology 1990;57:361—72.
[53] Kutala VK, Parinandi NL, Pandian RP, Kuppusamy P. Simultaneous measurement of oxygenation in intracellular and extracellular compartments of lung microvascular endothelial cells. Antioxidants and Redox Signalling 2004;6: 597—603.
[54] Subczynski W, Swartz H. EPR oxymetry in biological and model samples. In: Eaton S, Eaton G, Berliner L, editors. Biomedical ESR — Part A: free radicals, metals, medicine, and physiology, Vol. 23. Boston: Kluwer Academic Publishers; 2006.
[55] Brandis A, Salomon Y, Scherz A. Bacteriochlorophyll sensitizers in photodynamic therapy. In: Grimm B, Porra R, Rudiger W, Scheer H, editors. Chlorophylls and bacteriochlorophyls: biochemistry, biophysics, functions and applications. Dordrecht: Springer; 2006. p. 485—94.
[56] Katsumi TA, Aizawa K, Kuroiwa Y, Saito K, Kurata Y, Ii Y, et al. Photodynamic therapy with a diode laser for implanted fibrosarcoma in mice employing mono-L-aspartyl chlorin E6. Photochemistry and Photobiology 1996;64:671—5.
[57] Dabrowski JM, Urbanska K, Arnaut LG, Pereira MM, Abreu AR, Simoes S, et al. Biodistribution and photodynamic efficacy of a water-soluble, stable, halogenated bacteriochlorin against melanoma. ChemMedChem 2011;6:465—75.
[58] Mazor O, Brandis A, Plaks V, Neumark E, Rosenbach-Belkin V, Salomon Y, et al. WST11, a novel water-soluble bacteriochlorophyll derivative; cellular uptake, pharmacokinetics, biodistribution and vascular-targeted photodynamic activity using melanoma tumors as a model. Photochemistry and Photobiology 2005;81:342—51.

Please cite this article in press as: Jakubowska M, et al. Zinc-pheophorbide *a*—Highly efficient low-cost photosensitizer against human adenocarcinoma in cellular and animal models. Photodiagnosis and Photodynamic Therapy (2013), http://dx.doi.org/10.1016/j.pdpdt.2012.12.004